
In-Situ Measurements of High-Intensity Laser Beams on OMEGA

Introduction

Laser-driven, direct-drive inertial confinement fusion requires near-uniform illumination of the spherical fuel-bearing target;^{1,2} therefore, the target must be illuminated symmetrically since uneven illumination will result in uneven acceleration disrupting the implosion. For a laser-driven system with uniformly distributed beams, this dictates that all beams must have equal energies, must have the proper profile, and must be positioned accurately.

Currently, the primary method for determining the energies of beams on the OMEGA laser is based on a calorimeter system [harmonic energy diagnostic (HED)]. The beams must then be transported to the target chamber: they first pass through distributed polarization rotators (DPR's)³ and are then reflected off two mirrors and transmitted by a distributed phase plate (DPP),⁴ a focusing lens, and a vacuum window interface. Losses due to this transport are inferred from measurements made with a cw laser, but variations due to nonlinear effects at high power and variations of the beam shape are not otherwise measured. Likewise, the beam position is determined by a co-propagated cw laser, but with unknown positioning error (centroid determination of the reflected cw beam is accurate to 20 μm). With the method described here, relative beam fluence, shapes, and positions of the beams are determined from x-ray images of the emission from a 4-mm-diam, Au-coated spherical target illuminated by the beams of OMEGA.⁵ The UV light is converted to x rays in the Au coating with high efficiency,⁶ and the resultant x-ray flux is imaged with x-ray pinhole cameras (XPHC's) and recorded by charge-injection devices (CID's).⁷

This analysis takes into account projection effects, conversion from UV to x rays, and detection efficiency. This process is sufficiently automated to allow for analysis to be completed within the OMEGA minimum shot cycle (45 min). Mispositioned beams can be repointed to an accuracy of 9 μm (rms over 60 beams) again within a shot cycle. This method has also been used to determine and minimize beam-to-beam peak fluence

variations, thereby further improving on-target uniformity (enhanced fluence balance).⁸

On-Target Beam Measurements

The data present in XPHC images of pointing shots must be extracted and quantified. Ideally, the beams incident on the target are circularly symmetric and have a radial profile given by a "super-Gaussian" of the form

$$I_{\text{UV}}(r) = I_{\text{UV}}(0) \times e^{-(r/r_0)^\eta}, \quad (1)$$

where $I_{\text{UV}}(r)$ is the intensity of the beam as a function of radius, $I_{\text{UV}}(0)$ is the peak intensity, r is the distance from the beam center, r_0 is the beam-spot radius, and η is the power of the super-Gaussian.

The gold target converts the incident UV energy into x rays with a high efficiency.⁶ The result follows the proportionality⁸

$$I_x \propto I_{\text{UV}}^\gamma, \quad (2)$$

where I_x is the intensity of x rays produced by the target and γ is a constant. For the detectors used in this work,⁷ and a total filtration of 152 μm of Be, γ was estimated to be 3.7. X rays from the target are then imaged by XPHC's and recorded by CID cameras.

In general, the beams are not perfectly circular; therefore, they are fitted to an elliptical super-Gaussian. Combining Eqs. (1) and (2) and introducing an elliptical beam shape yields

$$I_x(r) = I_{\text{UV}}^\gamma(0) \times e^{-\gamma \left[(x'/a)^2 + (y'/b)^2 \right]^{\eta/2}}, \quad (3)$$

where a and b are the lengths of the major and minor axes of the ellipse, respectively. The values x' and y' are the coordinates

lying along the major and minor axes of the ellipse, given by

$$\begin{aligned} x' &= (x - x_c)\cos(\alpha) + (y - y_c)\sin(\alpha), \\ y' &= -(x - x_c)\sin(\alpha) + (y - y_c)\cos(\alpha), \end{aligned} \tag{4}$$

where x and y are the coordinates in the camera image, α is the phase angle of the ellipse, and x_c and y_c are the locations of the center of the beam in image coordinates.

The x-ray fluence measured by the CID cameras is then fit to Eq. (3), yielding values for the beam’s peak UV intensity, center position, super-Gaussian power, major and minor axes, and phase angle of the ellipse. Figure 100.31 shows a comparison of this fit to an actual XPHC image recorded by a CID

camera. The lineouts in Fig. 100.31(c) show an example comparison between measured and fit beam profiles.

1. Correction for Limb Brightening

As shown schematically in Fig. 100.32, x-ray emission from the Au plasma resulting from absorption of the UV beams is, in general, seen at an angle θ . If the emission comes from an optically thin medium, the increased path through the plasma will increase the observed x-ray fluence. It has been shown⁸ that when the plasma is uniform on the surface of the sphere, the intensity seen at an angle θ to the normal is given by

$$\begin{aligned} I_x(\theta) &= I_x(0)(r_{\text{emis}}/\Delta r) \\ &\times \left[\sqrt{1 + (\Delta r/r_{\text{emis}})^2 - \sin^2 \theta} - \cos \theta \right], \end{aligned} \tag{5}$$

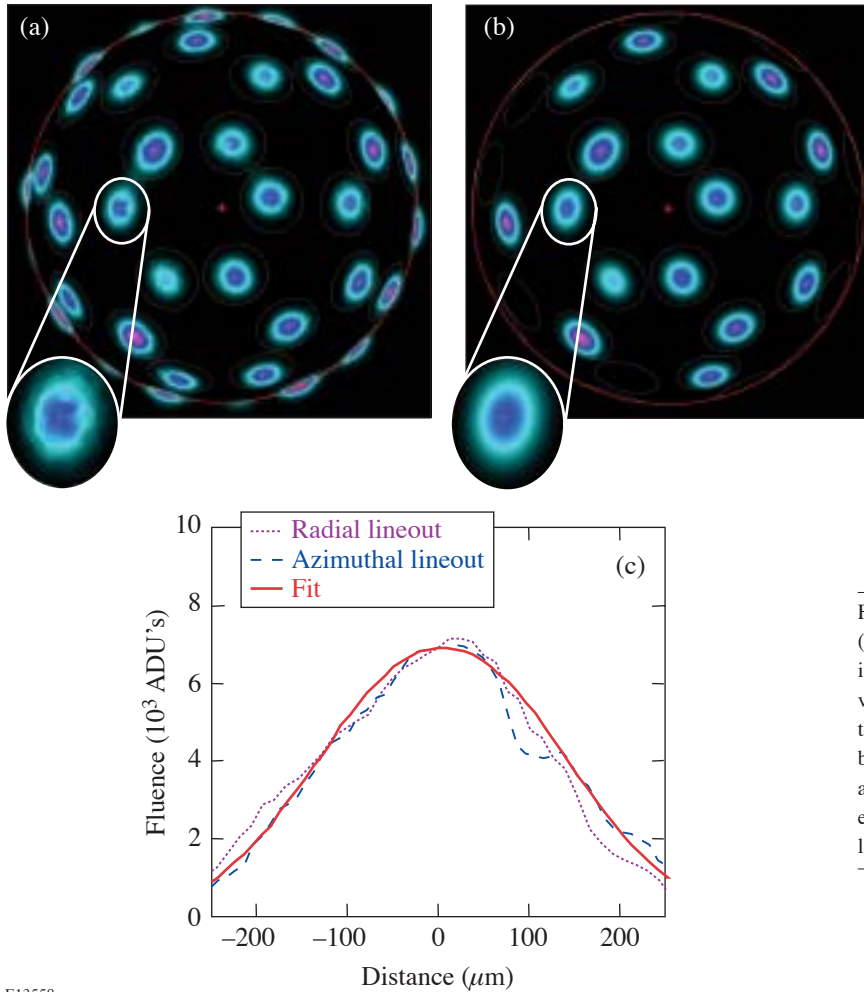


Figure 100.31
 (a) CID image of a 4-mm-diam, Au-coated pointing sphere illuminated by all 60 OMEGA beams with an enlarged view of beams 6 to 8. (b) The fit to this image created by the method described herein with an enlarged view of beams 6 to 8. Beams greater than 64° from the view center are not fit since they are greatly distorted by view-angle effects. (c) Radial and azimuthal lineouts compared to a lineout of the fit for beams 6 to 8.

E13558

where r_{emis} is the radius of the target and Δr is the thickness of the plasma. A typical value of $\Delta r = 113 \mu\text{m}$ was found on a uniformly irradiated, 1-mm-diam, Au-coated sphere with all other conditions the same as on a beam pointing shot (e.g., 1-ns square pulse at $\sim 10^{14} \text{W/cm}^2$). Correction for limb brightening on the pointing target is then accomplished by solving Eq. (5) for the value of $I_x(0)$, the intensity as seen from the normal to the target, using the values $\Delta r = 113 \mu\text{m}$ and $r_0 = 2 \text{mm}$. Since this correction is performed continuously for the entire x-ray image, the result is to approximately remove the effect of the curved surface on the measurements of beam fluence and beam position.

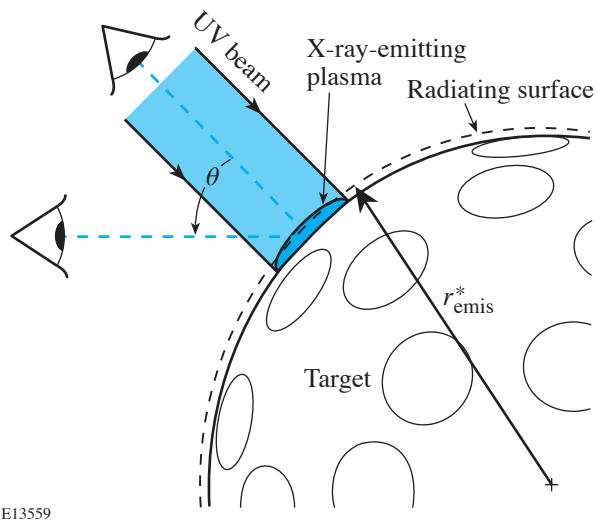


Figure 100.32
An OMEGA beam incident on a 4-mm-diam, Au-coated pointing target. The target will re-emit in the x-ray band with intensity and shape modified by conversion to x rays. However, since the beam is viewed by a camera off axis from the path of the beam, it appears to be distorted and to have a higher peak intensity than if it were viewed on axis, due to the limb-brightening effect. This also causes the apparent position of the beam on the radiating surface to be shifted from its actual position.

2. Determination of Beam Parameters

First, the images are fitted to a template of ideal beam positions (orthographic projections of beam-arrival directions), assuming the emission comes from the surface of a sphere [effective emission radius r_{emis}^* ; see Fig. (100.32)]. The best fit of this template to the observed beam positions then determines r_{emis}^* the target position and the orientation of the image with respect to target chamber coordinates (rotation angle).

After initial determination of the target position, radius, and image rotation angle, corrections for view angle are applied,

contributions from surrounding beams are removed, and the beam shape and position are recomputed. Typically this procedure is applied to images from a set of eight XPHC's located at the positions shown in Fig. 100.33. For each image, beams within 64° of the center position are analyzed. Therefore, all beams are viewed by two or more cameras, and error on beam position may be calculated by comparing determinations from multiple views. Application of the procedure described above gives improved results, as evidenced by a reduction of this error.

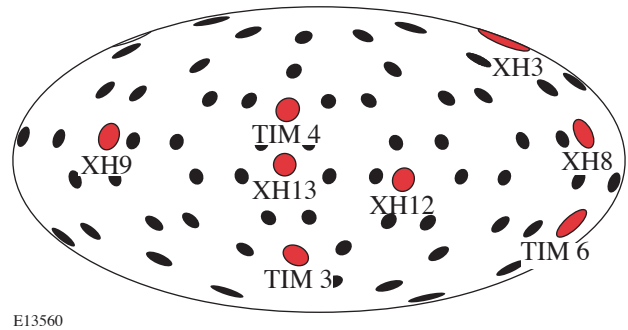


Figure 100.33
Aitoff projection plot of XPHC positions. The black circles represent beam positions. The red circles show the center position of each XPHC view, labeled with the viewport name.

After correction for projection effects, beam parameters may be measured with a high degree of accuracy. For any single SG3 beam on OMEGA, the radius may be determined to within 4%, ellipticity to within 4%, super-Gaussian power to within 4%, and peak fluence to within 4%. For a single SG4 beam, the radius may be determined to within 3%, ellipticity to within 2%, super-Gaussian power to within 6%, and peak fluence to within 4%. Differences between measurement accuracies for SG3 and SG4 beams are due to departures from the ideal beam shape.

This method has been used to determine the beam size, peak fluence variations, and pointing accuracy for the full 60 OMEGA beams when the beams are smoothed by 1-THz smoothing by spectral dispersion (SSD) with polarization smoothing (PS),⁹ both with the original DPP's (SG3) and with an expanded, flatter beam shape resulting from a new set of DPP's (SG4).¹⁰ The average beam shapes found from this analysis are $\eta = 2.27 \pm 0.02$ and $r_0 = 308 \pm 1 \mu\text{m}$ with ellipticity of 1.072 ± 0.005 for the SG3 beams, and $\eta = 3.66 \pm 0.03$ and $r_0 = 380 \pm 1 \mu\text{m}$ with ellipticity of 1.066 ± 0.003 for the SG4 beams. These

correspond to beam diameters of approximately $930\ \mu\text{m}$ and $865\ \mu\text{m}$ (diameter containing 95% of the energy) for the SG3 and SG4 DPP's, respectively.

3. Beam Repointing

Beam-position deviations from the desired template are determined from the final fits. The measured beam offsets are used to compute movements of the final turning mirrors, thereby correcting the pointing. Figure 100.34 shows the results of beam offset determinations before and after repointing (second pointing shot). The root-mean-square position error has been reduced from $23\ \mu\text{m}$ to $11\ \mu\text{m}$. This beam-repointing method has been applied many times, and the minimum rms position error achieved is $9\ \mu\text{m}$.

Conclusions

A method has been developed to accurately measure beam position, shape, and relative intensity from CID-recorded x-ray images of 4-mm-diam, Au-coated pointing targets irradiated with focused beams from the OMEGA laser. By taking into account projection effects, conversion from UV to x rays, and detection efficiency, this method is able to determine beam

position to within $7\ \mu\text{m}$, beam radius to within 3%, ellipticity to within 2%, and relative intensity to within 4%.

Accurate characterization of beams is necessary to optimize the uniformity of target illumination since displacements from ideal beam positions and variations in beam shape and intensity cannot be minimized unless they are first measured. This analysis is currently being used on OMEGA to improve the uniformity of target illumination by improving beam pointing.

ACKNOWLEDGMENT

This work was supported by the U.S. Department of Energy Office of Inertial Confinement Fusion under Cooperative Agreement No. DE-FC52-92SF19460, the University of Rochester, and the New York State Energy Research and Development Authority. The support of DOE does not constitute an endorsement by DOE of the views expressed in this article.

REFERENCES

1. J. Nuckolls *et al.*, *Nature* **239**, 139 (1972).
2. J. J. Duderstadt and G. A. Moses, *Inertial Confinement Fusion* (Wiley, New York, 1982), Chap. 1, pp. 7–8.

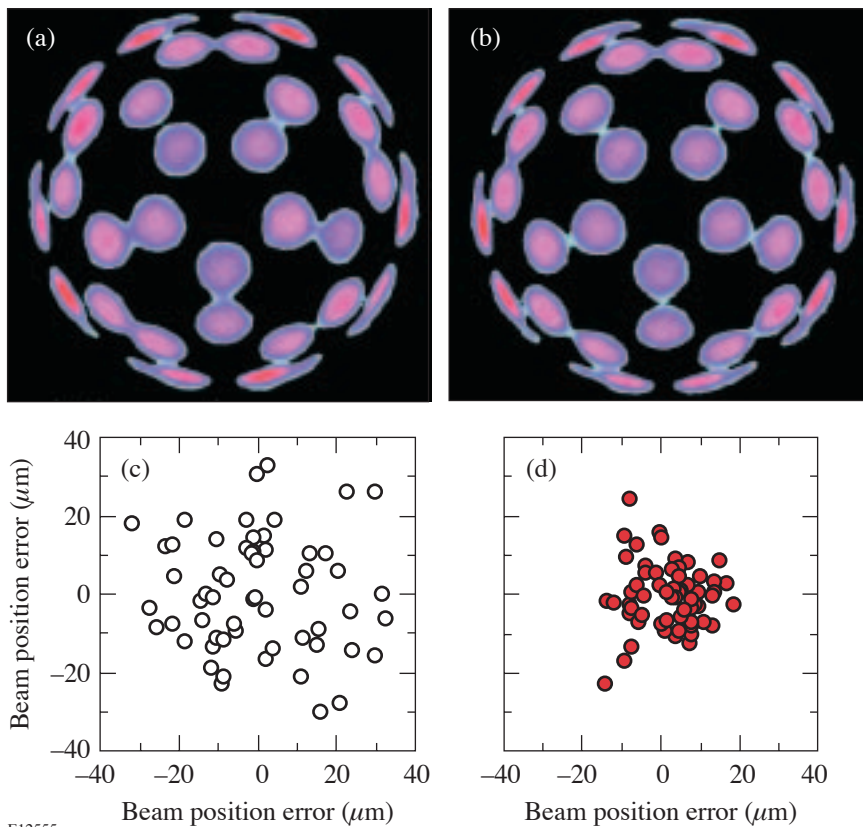


Figure 100.34

Result of repointing the OMEGA beams using the method described in this article. (a) XPHC image from the TIM 6 view showing beams before repointing. (b) XPHC image from the same view showing beams after repointing. Beam positions are visibly improved. (c) A plot of beam offsets from their ideal position before repointing. The root-mean-square offset is $23\ \mu\text{m}$. (d) A plot of beam offsets after repointing. The root-mean-square offset is reduced to $11\ \mu\text{m}$.

E12555

3. Laboratory for Laser Energetics LLE Review **45**, 1, NTIS document No. DOE/DP40200-149 (1990). Copies may be obtained from the National Technical Information Service, Springfield, VA 22161.
4. T. J. Kessler, Y. Lin, L. S. Iwan, W. P. Castle, C. Kellogg, J. Barone, E. Kowaluk, A. W. Schmid, K. L. Marshall, D. J. Smith, A. L. Rigatti, J. Warner, and A. R. Staley, in *Second Annual International Conference on Solid State Lasers for Application to Inertial Confinement Fusion*, edited by M. L. André (SPIE, Bellingham, WA, 1997), Vol. 3047, pp. 272–281.
5. J. M. Soures, R. L. McCrory, C. P. Verdon, A. Babushkin, R. E. Bahr, T. R. Boehly, R. Boni, D. K. Bradley, D. L. Brown, R. S. Craxton, J. A. Delettrez, W. R. Donaldson, R. Epstein, P. A. Jaanimagi, S. D. Jacobs, K. Kearney, R. L. Keck, J. H. Kelly, T. J. Kessler, R. L. Kremens, J. P. Knauer, S. A. Kumpan, S. A. Letzring, D. J. Lonobile, S. J. Loucks, L. D. Lund, F. J. Marshall, P. W. McKenty, D. D. Meyerhofer, S. F. B. Morse, A. Okishev, S. Papernov, G. Pien, W. Seka, R. Short, M. J. Shoup III, M. Skeldon, S. Skupsky, A. W. Schmid, D. J. Smith, S. Swales, M. Wittman, and B. Yaakobi, *Phys. Plasmas* **3**, 2108 (1996).
6. P. D. Goldstone, J. A. Cobble, A. Hauer, G. Stradling, W. C. Mead, S. R. Goldman, S. Coggeshall, M. C. Richardson, P. A. Jaanimagi, O. Barnouin, R. Marjoribanks, B. Yaakobi, F. J. Marshall, P. Audebert, and J. Knauer, in *X Rays from Laser Plasmas*, edited by M. C. Richardson (SPIE, Bellingham, WA, 1987), Vol. 831, pp. 54–61.
7. F. J. Marshall, T. Ohki, D. McInnis, Z. Ninkov, and J. Carbone, *Rev. Sci. Instrum.* **72**, 713 (2001).
8. F. J. Marshall, J. A. Delettrez, R. Epstein, R. Forties, R. L. Keck, J. H. Kelly, P. W. McKenty, S. P. Regan, and L. J. Waxer, *Phys. Plasmas* **11**, 251 (2004).
9. D. D. Meyerhofer, J. A. Delettrez, R. Epstein, V. Yu. Glebov, V. N. Goncharov, R. L. Keck, R. L. McCrory, P. W. McKenty, F. J. Marshall, P. B. Radha, S. P. Regan, S. Roberts, W. Seka, S. Skupsky, V. A. Smalyuk, C. Sorce, C. Stoeckl, J. M. Soures, R. P. J. Town, B. Yaakobi, J. D. Zuegel, J. Frenje, C. K. Li, R. D. Petrasso, D. G. Hicks, F. H. Séguin, K. Fletcher, S. Padalino, M. R. Freeman, N. Izumi, R. Lerche, T. W. Phillips, and T. C. Sangster, *Phys. Plasmas* **8**, 2251 (2001).
10. F. J. Marshall, J. A. Delettrez, R. Epstein, R. Forties, V. Yu. Glebov, J. H. Kelly, T. J. Kessler, J. P. Knauer, P. W. McKenty, S. P. Regan, V. A. Smalyuk, C. Stoeckl, J. A. Frenje, C. K. Li, R. D. Petrasso, and F. H. Séguin, *Bull. Am. Phys. Soc.* **48**, 56 (2003).